THE JOURNAL OF BIOLOGICAL CHEMISTRY VOL. 285, NO. 50, pp. 38933–38943, December 10, 2010

Inhibitors of Catalase-Amyloid Interactions Protect Cells from β-Amyloid-Induced Oxidative Stress and Toxicity*[S]

Received for publication, April 11, 2010, and in revised form, September 3, 2010 Published, JBC Papers in Press, October 5, 2010, DOI 10.1074/jbc.M110.132860

Lila K. Habib[‡1], **Michelle T. C. Lee**[§], **and Jerry Yang**[§2]

From the Departments of [‡]*Bioengineering and* [§]*Chemistry and Biochemistry, University of California, San Diego, La Jolla, California 92093-0358*

Compelling evidence shows a strong correlation between accumulation of neurotoxic β-amyloid (Aβ) peptides and oxidative stress in the brains of patients afflicted with Alzheimer disease (AD). One hypothesis for this correlation involves the direct and harmful interaction of aggregated Aβ peptides with enzymes responsible for maintaining normal, cellular levels of reactive oxygen species (ROS). Identification of specific, destructive interactions of Aβ peptides with cellular anti-oxidant enzymes would represent an important step toward understanding the pathogenicity of Aβ peptides in AD. This report demonstrates that exposure of human neuroblastoma cells to cytotoxic preparations of aggregated Aβ peptides results in significant intracellular co-localization of Aβ with catalase, an anti-oxidant enzyme responsible for catalyzing the degradation of the ROS intermediate hydrogen peroxide (H_2O_2). These catalase-Aβ interactions deactivate catalase, resulting in increased cellular levels of H_2O_2. Furthermore, small molecule inhibitors of catalase-amyloid interactions protect the hydrogen peroxide-degrading activity of catalase in Aβ-rich environments, leading to reduction of the co-localization of catalase and Aβ in cells, inhibition of Aβ-induced increases in cellular levels of H_2O_2, and reduction of the toxicity of Aβ peptides. These studies, thus, provide evidence for the important role of intracellular catalase-amyloid interactions in Aβ-induced oxidative stress and propose a novel molecular strategy to inhibit such harmful interactions in AD.

Although oxidative stress is commonly associated with aging (1, 2), patients with Alzheimer disease (AD)[3] often exhibit increased oxidative damage (3–10) and subsequent neuronal loss in β-amyloid (Aβ)-rich regions of the brain. The molecular mechanisms by which Aβ contributes to oxidative damage remain unclear (11–19). Understanding these mechanisms, however, is critical for developing effective methods to manage the disease. One mechanism for Aβ-induced cellular oxidative stress proposes that Aβ peptides interact directly with cellular enzymes responsible for maintaining low physiological levels of reactive oxygen species (ROS) (20–23). Two potential outcomes from such pathological protein-amyloid interactions are: 1) increased production of ROS, or 2) reduced degradation of ROS.

The major ROS in cells are superoxide and the more reactive hydrogen peroxide (H_2O_2)-derived hydroxyl radical (24, 25). Both superoxide and H_2O_2 are primarily produced in the mitochondria (26–28). Aβ peptides have been shown to accumulate in the mitochondria (29, 30), and, therefore, could exert their detrimental effects through interaction with mitochondrial proteins (23, 31–34). Superoxide is produced by several enzyme-catalyzed reactions in the mitochondria (25). Behl *et al.* (11) however, showed that a broad range of inhibitors of several of these enzymes had no effect on Aβ toxicity in clonal and primary neuronal cell cultures. Furthermore, Zhang *et al.* (35) reported that superoxide levels in cells were not substantially elevated upon exposure to Aβ. These findings suggest that superoxide is not a dominant contributor to Aβ toxicity.

On the other hand, Aβ-induced cellular increase in H_2O_2 or its metabolites is strongly correlated with Aβ toxicity (11, 13, 36). H_2O_2 can be generated by several mitochondrial enzymes including monoamine oxidases, superoxide dismutase, and xanthine oxidase (25). Behl *et al.* (11) showed that inhibitors of monoamine oxidases and xanthine oxidase had no effect on Aβ-induced H_2O_2 accumulation or Aβ toxicity. Gsell *et al.* (37) also found that the activity of superoxide dismutase was unaltered in the brains of AD patients. Additionally, Rensink *et al.* (38) reported that the Dutch mutation of Aβ peptides (HCHWA-D Aβ) did not bind directly to superoxide dismutase and Kaminsky *et al.* (39) reported only a relatively small effect of Aβ on superoxide dismutase activity and H_2O_2 production upon chronic exposure of rat brains to Aβ. These results suggest that Aβ peptides do not significantly affect production of H_2O_2 in cells. Consequently, these findings imply that Aβ-induced oxidative stress may arise from reduced degradation of H_2O_2 in Aβ-challenged cells.

Degradation of H_2O_2 in cells is primarily achieved by the enzymes catalase and glutathione peroxidase (GPx), both inside and outside of the mitochondria (25). Sagara *et al.* (40) found that cells resistant to Aβ toxicity had elevated levels of catalase and GPx. The activity of both enzymes was reduced in rat brains exposed to Aβ. In particular, Pappolla *et al.* and Lovell *et al.* found that catalase was associated with senile plaques in human brain sections from patients with AD (6, 41). Several groups have shown that transfection of cells with catalase (40) or addition of

* This work was supported in part by the Hellman Foundation, the Alzheimer Disease Research Center (3P50 AG005131), the Alzheimer Association (NIRG-08-91651), and the National Science Foundation (CAREER Award CHE-0847530, to J. Y.).

[S] The on-line version of this article (available at http://www.jbc.org) contains supplemental Figs. S1–S12 and other information.

[1] Supported by a Kuwait University fellowship.

[2] To whom correspondence should be addressed: 9500 Gilman Dr., MC 0358, La Jolla, CA 92093-0358. Tel.: 858-543-6006; Fax: 858-534-4554; E-mail: jerryyang@ucsd.edu.

[3] The abbreviations used are: AD, Alzheimer Disease; ROS, reactive oxygen species; Aβ, β-amyloid; GPx, glutathione peroxidase; BTA, 6-methylbenzothiazole aniline; EG, ethylene glycol; H_2O_2, hydrogen peroxide; SOD, superoxide dismutase.

catalase to the extracellular environment of cultured cells protected cells from Aβ toxicity (11, 38). This cytoprotective effect was attributed to a catalase-induced reduction of the H_2O_2 concentration outside and inside the cells, because H_2O_2 readily diffuses across cell membranes (25, 43). These observations are consistent with the hypothesis that H_2O_2, or its metabolites, but not superoxide, play a dominant role in Aβ-induced oxidative stress. Moreover, Milton *et al.* (21) and our previous work (55) revealed that Aβ binds directly to catalase in cell free assays, whereas Aβ does not bind to GPx (supplemental Fig. S12). The binding of Aβ to catalase leads to deactivation of the H_2O_2-degrading activity of catalase in solution (21). Evidence for direct catalase-amyloid interactions and their resulting detrimental effects within living cells, however, has not yet been reported. Testing the hypothesis that intracellular catalase-Aβ interactions play a significant role in Aβ-induced increases in cellular H_2O_2 may, therefore, provide a critical and missing mechanistic link between Aβ accumulation and oxidative stress in AD.

Here, we investigated the effect of catalase-amyloid interactions on Aβ-induced increases in H_2O_2 and on the resulting toxicity in live cells. In these studies, we exposed human neuroblastoma cells to a mixture of aggregated Aβ(1–42) peptides (containing soluble oligomers and protofibrils) to mimic the heterogeneous nature of aggregated Aβ species found in the brains of AD patients (44–46). Because the identity of the most toxic aggregated form of Aβ remains highly debated (47–53), we chose to use this mixture of different species of aggregated Aβ in these studies in order to increase the likelihood that as many toxic species as possible were included in all of our experiments. To assess whether catalase-amyloid interactions lead to Aβ-induced increases in H_2O_2 in cells, we designed and synthesized molecular probes with the following six characteristics: 1) capability of generating protein-resistant surface coatings on aggregated Aβ peptides (54–56) (to inhibit catalase-amyloid interactions in cells), 2) lack of toxicity, 3) cell permeability, 4) capability of accessing the same subcellular compartments of cells as Aβ, 5) intrinsic fluorescence properties (to visualize the intracellular location of the molecules), and 6) chemical stability in oxidizing environments. We achieved these characteristics with two oligo(ethylene glycol) derivatives of 6-methylbenzothiazole aniline (BTA-EG_4 and BTA-EG_6) (55); BTA analogs have well-known, high affinity binding properties to both Aβ oligomers and fibrils (57, 58). These molecules made it possible to challenge neuroblastoma cells with Aβ and to evaluate the effects of coating aggregated Aβ peptides with a protein-resistant surface on the viability of cells.

EXPERIMENTAL PROCEDURES

Materials—A detailed list of materials used in this research can be found in the supplemental information.

Preparation of Aggregated Aβ(1–42) Peptides—Aggregated Aβ(1–42) was prepared by incubation in deionized water (100 μM) at 37 °C for 72 h and characterized as described in the supporting information. For cellular experiments using aggregated Aβ, a stock solution of aggregated Aβ prepared in sterile water was diluted with an equivalent volume of 2× complete culture medium to create the desired concentration of aggregated Aβ dissolved in 1× complete medium. For cellular experiments using aggregated Aβ in the presence of the BTA-EG_x molecules, aggregated Aβ (in sterile water) was pre-incubated for 12 h with various concentrations of BTA-EG_4 or BTA-EG_6, followed by addition of an equal volume of 2× medium to create the desired solution of aggregated Aβ and BTA-EG_x dissolved in 1× medium.

MTT Cell Viability Assay—SH-SY5Y cells were plated at a density of 50,000 cells/well in 100 μl of complete medium consisting of a 1:1 mixture of Eagle's Minimum Essential Medium (EMEM) and Ham's F12, supplemented with 10% fetal bovine serum (FBS). Cells were incubated overnight before treatment with 100 μl of various sample solutions. Cells were exposed to solutions containing a final concentration of 25 μM Aβ and various concentrations of the BTA-EG_x molecules (0–40 μM) for 24 h at 37 °C. The MTT reagent (20 μl of the solution from the commercial kit) was added, and the cells were incubated for 3 additional hours. The cells were subsequently solubilized with detergent reagent (100 μl of the solution from the commercial kit) and incubated at room temperature overnight. The cell viability was determined by measuring the absorbance at 570 nm using a Spectramax 190 microplate reader (Molecular Devices). All results were expressed as percent reduction of MTT relative to untreated controls (defined as 100% viability), and the average absorbance value for each treatment was blanked with the absorbance reading of wells containing only medium, MTT reagent, and detergent reagent.

Measurement of Hydrogen Peroxide Release in Cells—Cells were plated in 50 μl of Dulbecco's modified Eagle's medium (DMEM) without phenol red, supplemented with 10% FBS and 4 mM L-glutamine. Cells were incubated overnight before dosing with sample solutions. The solutions of Aβ aggregates in the presence or in the absence of the BTA-EG_x molecules were incubated with the cells for 24 h. Cellular H_2O_2 release was determined by adding 20 μl/well of a solution containing 250 μM Amplex red reagent and 0.5 units/ml horseradish peroxidase (HRP) dissolved in complete medium. The absorbance at 560 nm was subsequently measured 30 min after addition of the Amplex red/HRP solution (59). For control experiments, cells were incubated for 24 h with 40 μM BTA-EG_x, 20 mM 3AT, or 20 mM 3AT with 40 μM BTA-EG_x, followed by measurement of H_2O_2 released. All absorbance measurements for each treatment were measured in triplicate and the average absorbance values of control wells containing medium alone were subtracted.

Immunofluorescence Analysis of the Cellular Co-localization of Aβ and Catalase—SH-SY5Y cells were cultured on poly-L-lysine coated glass cover slips and incubated overnight in a 1:1 mixture of EMEM and Ham's F12 supplemented with 10% FBS. The growth medium was removed and solutions of aggregated fluorescently labeled Aβ (5 μM dissolved in medium), or fluorescently labeled Aβ (5 μM) that had been pre-incubated with BTA-EG_x (40 μM), were added to the different glass cover slips. The cells were incubated for 12 h. To visualize co-localization of aggregated Aβ with catalase, the cells were fixed with 4% paraformaldehyde in PBS (pH 7.4) and permeabilized with 0.25% Triton-X in PBS, followed by incubation with a rabbit anti-catalase polyclonal antibody on a

shaker at 4 °C overnight. To detect the primary antibody, a fluorescently labeled goat anti-rabbit antibody (diluted 1:1000) was added to the glass slides and incubated in the dark, on a shaker at room temperature for 2 h. Coverslips were mounted using Hydromount mounting medium (product no. HS-106) from National Diagnostics (Atlanta, GA) according to the manufacturers guidelines and allowed to dry for 48 h in the dark at 4 °C before imaging with a Delta Vision Deconvolution Microscope System (Applied Precision, Issaquah, WA) equipped with a Nikon TE-200 inverted light microscope, with infinity corrected lenses, and with a mercury arc lamp as the illumination source. The fluorescence of the HiLyte Fluor 488-labeled Aβ (Abs/Em: 503/528 nm) was detected using an Ex/bp: 490/20 nm excitation filter and an Em/bp: 528/38 nm emission filter. The fluorescence of the Alexa Fluor 647 goat anti-rabbit antibody (Abs/Em: 650/668) was monitored using an Ex/bp: 640/20 nm excitation filter and an Em/bp: 685/40 nm emission filter. The co-localization was visualized and Pearson's correlation coefficient of the entire three-dimensional volume of the cell was determined using softWoRx image analysis software (Applied Precision, Issaquah, WA). The images shown in Fig. 3 are fluorescence micrographs of representative z-slices within cells.

Co-immunoprecipitation of Aβ with Catalase—SH-SY5Y cells were grown to confluence on 10-cm tissue culture-treated dishes. The medium was removed, and solutions of aggregated Aβ(1–42) (25 μM, in medium), Aβ (25 μM) that had been preincubated with BTA-EG_x (40 μM) or fresh medium were added to the different dishes and incubated overnight. The solutions were removed, and the cells were carefully washed three times with ice-cold PBS. The cells were incubated with 1 ml of ice-cold lysis buffer (from Cell Signaling Technology, Inc, Danvers, MA, Product No: 9803) containing a protease inhibitor mixture (Sigma-Aldrich, Product No: P2714) and 1 mM phenylmethylsulfonyl fluoride and placed on a shaker for 30 min at 4 °C. The cell lysate was collected, centrifuged, and the supernatant of the sample was precleared with 50 μl of protein G-agarose beads (Roche Diagnostics Co., Indianapolis, IN, Product No: 11719416001) to remove proteins that bind nonspecifically to protein G. The precleared cell lysate was subjected to immunoprecipitation with a goat polyclonal to catalase antibody (Abcam Inc., Cambridge, MA, Product No: ab50434) and protein G-agarose beads were used to extract the anti-catalase antibody and catalase from the lysate. The samples were subjected to 4–12% SDS-polyacrylamide gel electrophoresis. Catalase (from human erythrocytes) and synthetic aggregated Aβ(1–42) were also separated on the same gel as the immunoprecipitated proteins for comparison purposes. Western blot analyses using rabbit polyclonal anti-catalase antibody (Abcam Inc., Product No: ab1877) and 6E10 monoclonal anti-Aβ(1–16) antibody (Covance) were performed. Chemiluminescence was used to detect the proteins.

Assessment of the Cellular Internalization of Aβ and BTA-EG_x Molecules by Fluorescence Deconvolution Microscopy—SH-SY5Y cells were plated in DMEM without phenol red (supplemented with 10% FBS and 4 mM L-glutamine) on 35 mm glass bottom dishes (MatTek Co., Ashland, MA) and incubated overnight. The growth medium was removed, and solutions of pre-aggregated fluorescently labeled Aβ (5 μM dissolved in medium) with or without BTA-EG_x (40 μM dissolved in medium) were added to the cells and allowed to incubate for 12 h before imaging. The cells were washed with DMEM (without phenol red or FBS) immediately prior to imaging with a Delta Vision Deconvolution Microscope System (Applied Precision, Issaquah, WA) equipped with a Nikon TE-200 inverted light microscope, with infinity corrected lenses, and with a mercury arc lamp as the illumination source. The co-localization was determined using softWoRx image analysis software (Applied Precision, Issaquah, WA). The intrinsic fluorescence of the BTA-EG_x molecules (Abs/Em: 360/440 nm (60)) was observed by excitation with bandpass (bp) filtered light (Ex/bp: 360/40 nm) and the emission monitored at Em/bp: 457/50 nm. The fluorescence of the HiLyte Fluor 488-labeled Aβ (Abs/Em: 503/528 nm) was detected using an Ex/bp: 490/20 nm excitation filter and an Em/bp: 528/38 nm emission filter. The images shown in Fig. 5 are fluorescence micrographs of representative z-slices within cells.

Flow Cytometry—SH-SY5Y cells were grown to confluence on 35 mm tissue culture-treated dishes. The medium was removed, and solutions of aggregated fluorescently labeled Aβ (5 μM dissolved in medium), fluorescently labeled Aβ (5 μM) that had been preincubated with BTA-EG_x (40 μM), or fresh medium only were added to different dishes, and incubated overnight. The solutions were removed, and the cells were carefully washed with PBS. The cells were dissociated from the tissue culture dishes with solutions of 0.25% trypsin-EDTA, collected, and counted. The dead cells in each sample were stained using Live/Dead fixable far red stain (Invitrogen Co., Product No: L10120) according to the manufacturer's protocol, and all cell samples were fixed with 4% paraformaldehyde in PBS (pH 7.4). The flow cytometry data were acquired using a FACSCanto flow cytometer (Becton Dickinson, San Jose, CA) equipped with an argon 488 nm laser and a 530/30 band-pass filter to analyze the fluorescently labeled Aβ as well as a helium-neon 633 nm laser and a 660/20 band-pass filter to analyze the far red dye. FACSDiva software (Becton Dickinson) was used to control the setup, acquisition, and analysis of flow cytometry data from the FACSCanto flow cytometer. The samples were gated to only include single cell populations, excluding larger cell aggregates and cellular debris. This population contained more than 95% viable cells (>20,000 cells/sample). The live cells were analyzed for the presence of fluorescently labeled Aβ, and the cellular fluorescence from this cell population was presented as histograms.

Measurement of Catalase Activity in the Presence of Aggregated Aβ or Preincubated Samples of Aggregated Aβ with BTA-EG_x Molecules—The wells of 96-well plates were charged with 48-μl solutions containing final concentrations of 25 μM aggregated Aβ (in water) and 0–100 μM BTA-EG_x (in 1% DMSO/1% BSA in 50 mM sodium phosphate buffer). After shaking for 12 h, 15 μl of a catalase solution was added to give a final concentration of 25 nM catalase. The mixture was placed on a shaker for 2 additional hours. The activity of catalase was determined by adding 15 μl of a solution containing 5 μM HRP, 435 μM 4-aminoantipyrine (AP) and 435

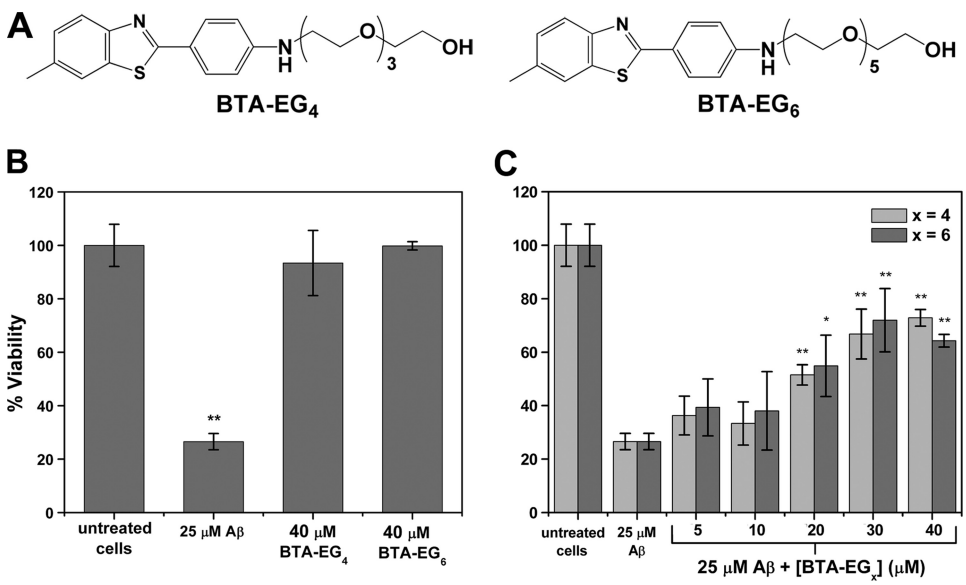

FIGURE 1. **Effect of aggregated Aβ(1–42) on the viability of SH-SY5Y cells and the cytoprotective effects of BTA-EG$_x$ against Aβ toxicity.** *A*, structures of BTA-EG$_4$ and BTA-EG$_6$. *B*, viability of cells in the presence of 25 μM aggregated Aβ or 40 μM BTA-EG$_x$ compared with untreated cells (**, $p < 0.01$ compared with untreated control cells). Cells were exposed to Aβ or BTA-EG$_x$ for 24 h. *C*, protection of cell viability in the presence of 25 μM aggregated Aβ that was pre incubated with various concentrations of BTA-EG$_x$. Data are expressed as mean values ± S.D., $n = 3$ for each concentration. *, $p < 0.05$ or **, $p < 0.01$ compared with cells incubated with 25 μM Aβ alone (*i.e.* in the absence of small molecules).

μM 3,5-dichloro-2-hydroxybenzenesulfonic acid (DHBS) (HRP, AP, and DHBS collectively are hereby defined as the colorimetric reagents) to the wells, immediately followed by 15 μl of 3 mM H_2O_2 (in 50 mM sodium phosphate buffer, pH 7.4). Catalase activity was monitored 10 min after the addition of H_2O_2 by measuring the absorbance at 505 nm (61, 62). The average absorbance values for each concentration of BTA-EG$_x$ were subtracted with the absorbance value of blanks consisting of 25 μM Aβ, the corresponding concentration of the BTA-EG$_x$ molecules, 25 nM catalase, the colorimetric reagents, and 50 mM sodium phosphate buffer (instead of a solution of H_2O_2). The results were expressed relative to absorbance values measured when catalase was not exposed to Aβ (defined as 100% catalase activity), and the absorbance measured when the assay was run in the absence of catalase (defined as 0% catalase activity).

RESULTS

BTA-EG$_x$ Molecules Reduce the Toxicity of Aβ Peptides—We hypothesized that small molecules (*e.g.* BTA-EG$_x$, Fig. 1*A*) with the capability of forming protein-resistant surface coatings on aggregated Aβ peptides (55) could protect cells from Aβ toxicity. To test this hypothesis, we determined the viability (63, 64) of human SH-SY5Y neuroblastoma cells after exposure to aggregated Aβ peptides in the presence or in the absence of these small molecules. For these experiments, we mimicked the heterogeneous population of aggregated Aβ species in AD brains (44–46) by using a preparation of Aβ peptides that contained ~15% small oligomers (MW ~15 kDa corresponding to trimers), ~25% medium-sized oligomers (MW 20–65 kDa corresponding to 5–15 mers), and ~60% soluble protofibrils (MW > 150 kDa corresponding to > 30 mers) (see supplemental Fig. S1). Fig. 1*B* shows that exposure of cells to 25 μM concentrations of this Aβ preparation reduced their viability to ~27% compared with control cells that were cultured in the absence of Aβ.

Before exploring the effect of the BTA-EG$_x$ molecules on reducing the cytotoxicity of Aβ, we tested the tolerance of cells to these BTA-EG$_x$ molecules by themselves. These experiments revealed that the BTA-EG$_x$ molecules were not toxic at concentrations up to 40 μM[4] (Fig. 1*B* and supplemental Fig. S2). Remarkably, the BTA-EG$_x$ molecules were, however, capable of reducing the toxicity of aggregated Aβ, causing an increase in cell viability to ~72% (Fig. 1*C*).[5] Because we used a mixture of aggregated Aβ species in these experiments, the results shown in Fig. 1*C* suggest that the BTA-EG$_x$ molecules could simultaneously protect cells from several potentially toxic forms of aggregated Aβ peptides that are present in this mixture (47–53). In all of the work shown here, we describe results using both of the structurally related BTA-EG$_4$ and BTA-EG$_6$ molecules because testing two molecules provides 2-fold evidence that this class of molecules can protect cells from Aβ-related injury.

[4] Further examination showed that these molecules are not toxic to this cell line at concentrations below 60 μM (supplemental Fig. S2).

[5] Interestingly, when SH-SY5Y cells are preincubated with the BTA-EG$_x$ molecules for 24 h prior to challenging cells with untreated aggregated Aβ peptides (i.e., aggregated Aβ that was not preincubated with BTA-EG$_x$), we did not observe significant inhibition of Aβ-induced toxicity in the cells. Because the effect of the BTA-EG$_x$ molecules on protection of Aβ-induced toxicity in cells depended on whether they were preincubated with the aggregated Aβ prior to exposure of the peptides to the cells, we hypothesize that distribution of the BTA-EG$_x$ molecules in cells may be different depending on whether they are introduced to cells alone (i.e., in the absence of Aβ) or whether the BTA-EG$_x$ molecules are preincubated and introduced to cells together with Aβ peptides. Preincubation with Aβ may, therefore, improve internalization of the BTA-EG$_x$ molecules and facilitate, enhance, or stabilize intracellular interactions between BTA-EG$_x$ and Aβ.

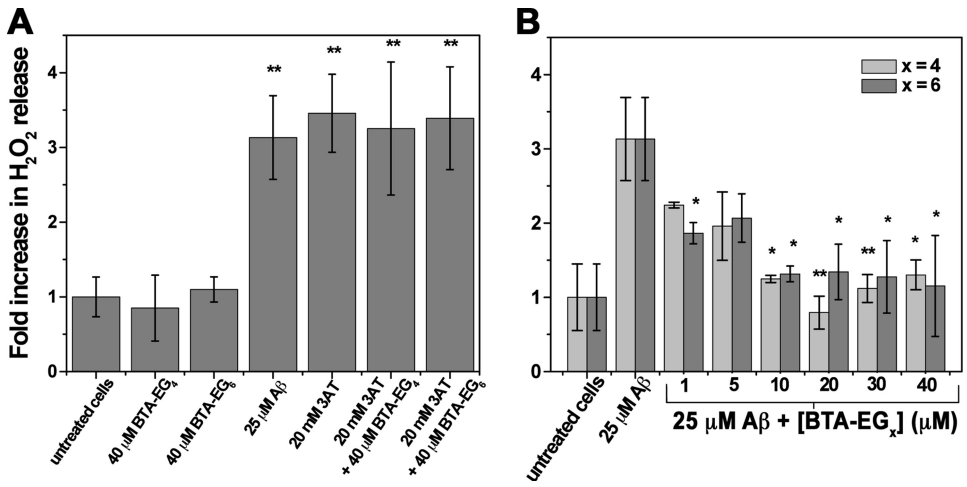

FIGURE 2. **Detection of Aβ-induced increase in release of H_2O_2 from SH-SY5Y cells.** *A*, H_2O_2 release from SH-SY5Y cells alone, or treated with BTA-EG_x, aggregated Aβ, catalase inhibitor 3AT, or a combination of 3AT and BTA-EG_x (**, $p < 0.01$ compared with untreated control cells). *B*, H_2O_2 release from SH-SY5Y cells treated with aggregated Aβ peptides that were preincubated with 1–40 μM concentrations of BTA-EG_x. Results are reported relative to the H_2O_2 concentration released by untreated cells. *, $p < 0.05$ or **, $p < 0.01$ compared with cells treated with 25 μM Aβ alone. Data are expressed as mean values ± S.D., $n = 3$ for each concentration.

BTA-EG_x Molecules Inhibit Aβ-induced Increases in Cellular H_2O_2 Levels—To assess whether the BTA-EG_x molecules can minimize Aβ-induced increases in cellular H_2O_2 levels, we measured the amount of H_2O_2 released by SH-SY5Y cells in the presence of aggregated Aβ peptides. Fig. 2*A* demonstrates that cells incubated with 25 μM Aβ for 1 day released 3-fold more H_2O_2 than control cells that were not exposed to Aβ. Moreover, Fig. 2*B* shows that concentrations of BTA-EG_x above 10 μM significantly inhibited Aβ-induced elevations in H_2O_2 levels in these cells. The presence of the BTA-EG_x molecules together with Aβ resulted in low H_2O_2 levels that were indistinguishable from control cells. Additional control experiments showed that 40 μM solutions of the BTA-EG_x molecules by themselves (*i.e.* in the absence of Aβ) did not affect cellular H_2O_2 levels compared with cells that were not exposed to these small molecules (Fig. 2*A*).

To evaluate if the BTA-EG_x molecules exerted their action by either specifically inhibiting Aβ-induced increases in cellular H_2O_2 levels or by reacting chemically with H_2O_2 or other ROS, we inhibited catalase with a known inhibitor (3-amino-1,2,4-triazole, 3AT (25, 65)). We expected this treatment to increase cellular levels of H_2O_2. Fig. 2*A* shows that a 20 mM solution of 3AT caused a 3-fold increase in H_2O_2 released by cells compared with untreated control cells. This increase in H_2O_2 levels was not affected by incubating cells with 3AT in the presence of 40 μM BTA-EG_x (Fig. 2*A*), demonstrating that the anti-oxidant properties of the BTA-EG_x molecules are specific to Aβ-mediated oxidative stress. Mass spectrometry analysis provided additional evidence that the BTA-EG_x molecules did not react directly with H_2O_2 in solution (see supplemental information). The BTA-EG_x molecules, therefore, exerted their activity by a mechanism that is different from a chemical anti-oxidant mechanism.

BTA-EG_x Molecules Readily Internalize in Cells and Reduce the Intracellular Co-localization of Aβ and Catalase—To test the hypothesis that intracellular protein-amyloid interactions contribute to Aβ-induced increases in H_2O_2 levels and to Aβ toxicity in live cells, we exposed SH-SY5Y cells to a solution containing N-terminal, fluorescently labeled Aβ peptides. This experiment made it possible to determine the location of these peptides inside of cells. Fig. 3, *A–D* and supplemental Figs. S3 and S4 illustrate that aggregated Aβ(1–42) peptides readily enter live cells and distribute to multiple subcellular

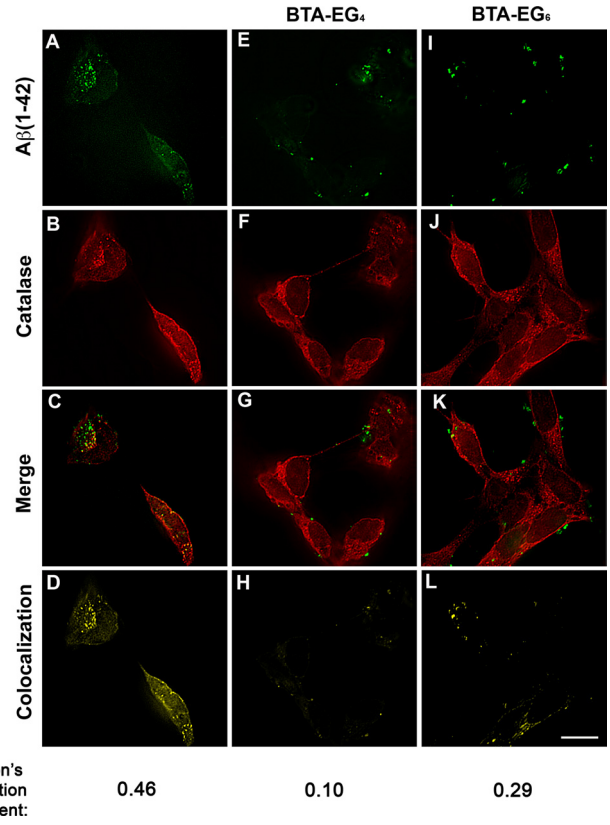

FIGURE 3. **Co-localization of aggregated Aβ(1–42) with catalase in SH-SY5Y cells.** *A–D*, fluorescence micrographs of representative z-slices within a cell show the co-localization of fluorescently-labeled aggregated Aβ peptides (*A*, *green*) with catalase (*B*, *red*). *C* represents a merged image of *A* and *B*. *D*, represents the areas of co-localization of *A* and *B* (*yellow*). *E–H* and *I–L* fluorescence micrographs of representative z-slices within a cell illustrating the reduced co-localization of Aβ peptides and catalase in the presence of the BTA-EG_x molecules. Scale bar, 10 μm.

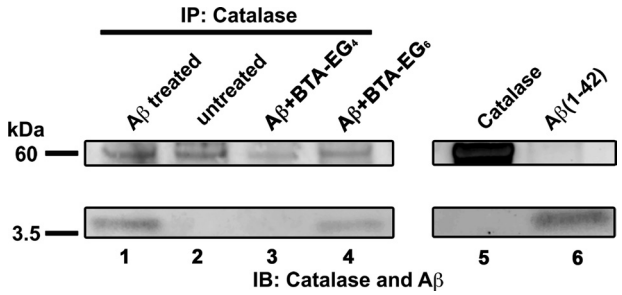

FIGURE 4. **Co-immunoprecipitation of Aβ(1–42) with catalase in the presence or absence of the BTA-EG$_x$ molecules.** SH-SY5Y cells that were treated with: (i) 25 μM Aβ (1–42) (*lane 1*), (ii) neither Aβ (1–42) nor the BTA-EG$_x$ molecules (*lane 2*), (iii) 25 μM Aβ preincubated with 40 μM BTA-EG$_4$ (*lane 3*), and (iv) 25 μM Aβ preincubated with 40 μM BTA-EG$_6$ (*lane 4*). All cells were immunoprecipitated with an anti-catalase antibody and subjected to Western blot analysis with anti-Aβ and anti-catalase antibodies. Catalase from human erythrocytes (*lane 5*) and pure Aβ(1–42) (*lane 6*) were also separated and stained on the same immunoblot (*IB*).

locations such as the lysosomes (supplemental Fig. S3) and mitochondria (supplemental Fig. S4). Because catalase is the primary enzyme responsible for degradation of H_2O_2 in cells (25, 71), we investigated whether the interaction of Aβ peptides with intracellular catalase (72) could contribute to the observed Aβ-induced increase in H_2O_2 levels. Fig. 3, *A–D* and supplemental Fig. S5 show that a significant fraction of the aggregated Aβ(1–42) peptides co-localized with catalase in the peroxisomes and in the cytosol; this observation has not been reported previously in live cells (30, 33, 66–70). Fig. 3 also shows that BTA-EG$_4$ (Fig. 3*H*) and BTA-EG$_6$ (Fig. 3*L*) significantly reduced the intracellular co-localization of Aβ and catalase. Although Fig. 3 shows only representative z-slice fluorescence micrographs of these cells, we quantified the degree of co-localization of Aβ and catalase within the entire three-dimensional volume of cells with the Pearson's correlation coefficient (73). Before addition of the BTA-EG$_x$ molecules, this coefficient was 0.46, whereas it was 0.10 or 0.29 when cells were introduced to Aβ together with BTA-EG$_4$ or BTA-EG$_6$, respectively. The molecular association between Aβ(1–42) peptides and catalase was further supported by exposing SH-SY5Y cells to aggregated Aβ(1–42) peptides and immunoprecipitating catalase with an anti-catalase antibody. Western blot analysis revealed a protein band of ~4.5 kDa in the lysates (corresponding to the MW of Aβ monomers), which was immunoreactive to an anti-Aβ antibody and co-immunoprecipitated with catalase (one subunit ~60 kDa) (Fig. 4). This ~4.5 kDa band was not observed in the Western blots from control cells that were not treated with Aβ. Additionally, immunoprecipitation of catalase in the presence of the BTA-EG$_x$ molecules reduced the co-immunoprecipitation of Aβ peptides with the catalase from the cell lysate (Fig. 4). Interestingly, the fluorescence microscopy experiments and the co-immunoprecipitation experiments revealed a consistent trend for the slightly better performance of BTA-EG$_4$ for reducing the interaction of Aβ with catalase in cells compared with the BTA-EG$_6$. We attribute this apparent enhanced performance of BTA-EG$_4$ to its increased lipophilicity compared with BTA-EG$_6$ (55), which may facilitate internalization in cells.

As a control for the fluorescence microscopy co-localization experiment, we also investigated the possible intracellular interaction of aggregated Aβ peptides with superoxide dismutase (SOD). Supplemental Fig. S6 shows results from fluorescence confocal imaging experiments revealing a reduced degree of overlap of aggregated Aβ and SOD throughout the entire volume of the cell (Pearson's coefficient = 0.27) relative to the overlap of Aβ and catalase (Pearson's coefficient = 0.46) under the same conditions. Additionally, the presence of the BTA-EG$_x$

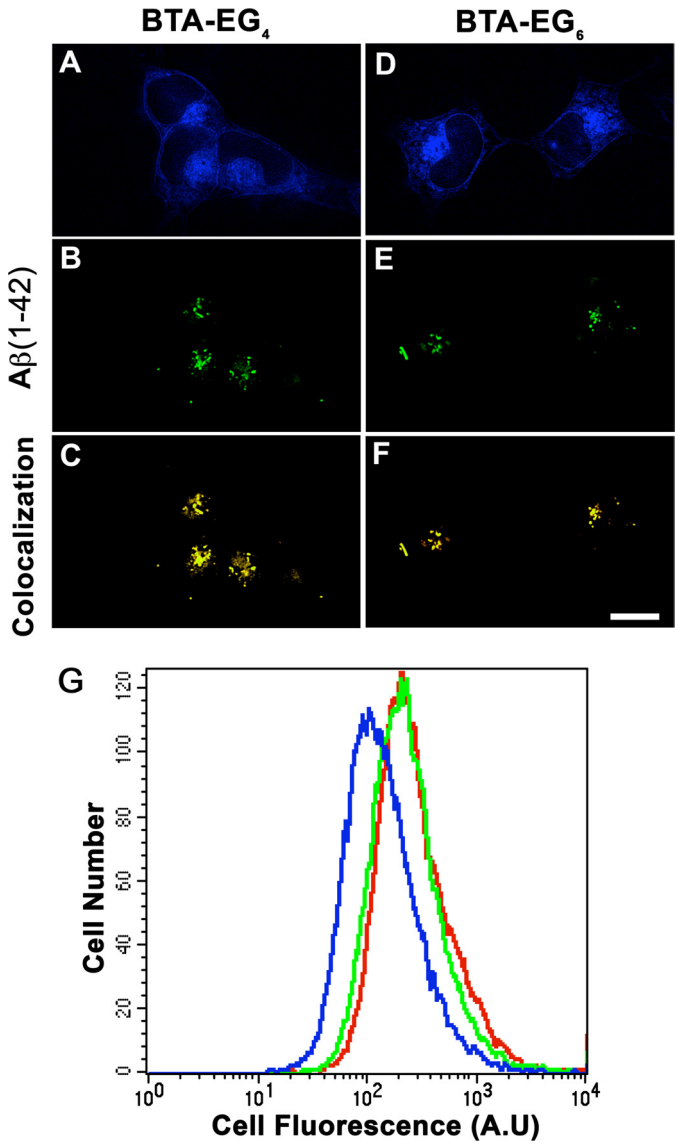

FIGURE 5. **Internalization of aggregated Aβ(1–42) and BTA-EG$_x$ molecules by SH-SY5Y cells.** *A–C*, fluorescence micrographs of representative z-slices within a cell showing that BTA-EG$_4$ (*A*, *blue*) and fluorescently labeled aggregated Aβ peptides (*B*, *green*) internalize in SH-SY5Y cells. *C* represents areas of co-localization of Aβ with BTA-EG$_4$ (*yellow*). *D–F*, fluorescence micrographs of representative z-slices within a cell showing that BTA-EG$_6$ (*D*, *blue*) and fluorescently-labeled aggregated Aβ peptides (*E*, *green*) internalize in SH-SY5Y cells. *F* represents areas of co-localization of Aβ with BTA-EG$_6$ (*yellow*). Scale bar, 10 μm. *G*, effect of BTA-EG$_x$ molecules on the cellular uptake of aggregated, fluorescently labeled Aβ(1–42) in SH-SY5Y cells. The histograms show the number of SH-SY5Y cells as a function of their total fluorescence intensity that were incubated with: (i) 5 μM fluorescently labeled Aβ (*red curve*) (ii) 5 μM fluorescently labeled Aβ preincubated with 40 μM BTA-EG$_4$ (*green curve*), or (iii) 5 μM fluorescently labeled Aβ preincubated with 40 μM BTA-EG$_6$ (*blue curve*) for 24 h. Data were generated by flow cytometry analysis of individual cells (>20,000 cells per sample). Statistical analysis of the data revealed that there was no significant difference in the cellular uptake of Aβ(1–42) incubated with or without the BTA-EG$_x$ molecules.

molecules did not affect the degree of overlap of Aβ and SOD (Pearson's coefficient = 0.30 for both BTA-EG_x molecules) compared with cells that were treated with Aβ alone (supplemental Fig. S6). Finally, we exposed SH-SY5Y cells to aggregated Aβ(1–42) peptides and immunoprecipitated SOD with an anti-SOD antibody. These experiments reveal that SOD does not appear to co-immunoprecipitate with Aβ (supplemental Fig. S7), which is in contrast to the observed co-immunoprecipitation of Aβ with catalase under the same conditions (Fig. 4). These results support that Aβ and SOD do not likely interact significantly within cells.

Fig. 3 and supplemental Fig. S5 clearly illustrates that the BTA-EG_x molecules are capable of reducing the co-localization of catalase and Aβ in cells. To test if this effect could be due to the interaction of the BTA-EG_x molecules with Aβ, we determined whether the BTA-EG_x molecules could also interact with Aβ in the cells. Fig. 5, *A–F* shows that the intrinsically fluorescent (60) BTA-EG_x molecules distributed throughout the cells and can occupy overlapping subcellular regions of the cells that are also occupied by Aβ. Additionally, Fig. 5*G* shows results from flow cytometry experiments demonstrating that the BTA-EG_x molecules (especially BTA-EG_4) do not significantly affect the uptake of the aggregated fluorescently labeled Aβ peptides in the cells. These results are consistent with the possibility that the BTA-EG_x molecules were capable of entering cells and could, hence, interact with intracellular pools of Aβ peptides. We hypothesize that this interaction between the BTA-EG_x molecules and Aβ protected cells from harmful protein-amyloid interactions by forming protein-resistant molecular surface coatings on Aβ (55). Such a mechanism would explain the observed reduction in intracellular co-localization of catalase and Aβ in the presence of the BTA-EG_x molecules. To test this hypothesis, we examined whether the BTA-EG_x molecules protected the H_2O_2-degrading activity of catalase in Aβ-rich environments.

BTA-EG_x Molecules Protect the H_2O_2-degrading Activity of Catalase in the Presence of Aβ—We reported previously that BTA-EG_4 and BTA-EG_6 could inhibit catalase-Aβ binding interactions in solution by forming protein-resistant surface coatings on aggregated Aβ(1–42) peptides (55). In order to determine whether these molecules could also protect the enzymatic activity of catalase in an Aβ-rich environment, we developed an assay for quantifying catalase activity (see supplemental Fig. S8). We designed this assay to be compatible with the presence of the BTA-EG_x molecules and with the presence of aggregated Aβ peptides in solution (see supplemental Fig. S9). Fig. 6*A* shows that micromolar concentrations of Aβ suppressed catalase activity substantially, in agreement with previous reports (21). Importantly, Fig. 6, *B* and *C* shows that the presence of BTA-EG_x molecules preserved 80–90% of catalase activity despite the presence of Aβ. The concentration of BTA-EG_x molecule that resulted in half-maximal preservation of catalase activity was ~8 nM for BTA-EG_4 and ~40 nM for BTA-EG_6.[6] These results are consistent

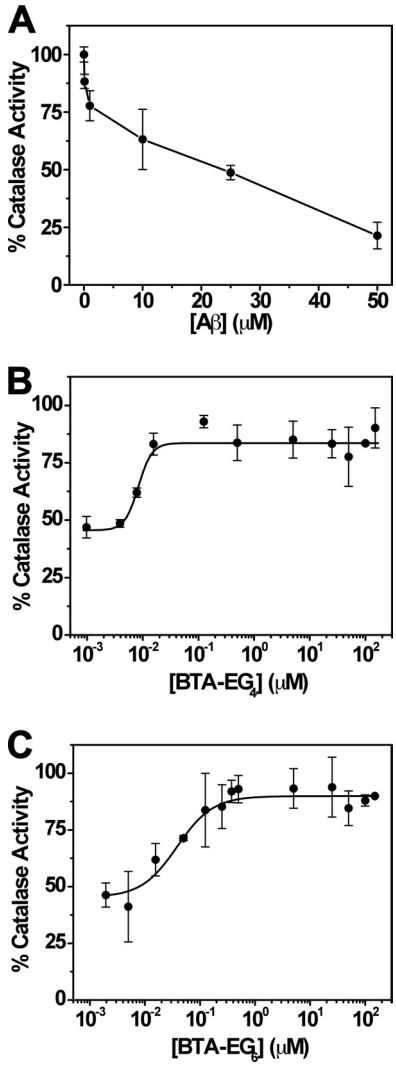

FIGURE 6. **Inhibition of catalase activity by Aβ and preservation of catalase activity by BTA-EG_x molecules in Aβ-rich solutions.** *A*, catalase activity in the presence of increasing concentrations of aggregated Aβ. The results are expressed relative to activity of catalase in the absence of Aβ. *B* and *C*, catalase activity in the presence of presence of 25 μM aggregated Aβ and increasing concentrations of BTA-EG_4 (*B*) or BTA-EG_6 (*C*). Catalase activity was defined as 100% when no Aβ was present and as 0% when no catalase was present in the sample. Data are expressed as mean values ± S.D., $n = 4$ for each concentration.

with the hypothesis that the BTA-EG_x molecules protect cells from Aβ-induced increases in H_2O_2 levels and from Aβ toxicity through a mechanism involving the formation of protein-resistant molecular coatings on aggregated Aβ.[7]

[6] Repeating the experiments used to generate the data shown in Fig. 6, *B* and *C* revealed variation of roughly an order of magnitude in the estimation of IC_{50} values for BTA-EG_x, suggesting there is no significant difference in the potency between BTA-EG_4 and BTA-EG_6 in this cell-free assay.

[7] We attribute the differences in required concentrations of BTA-EG_x, either to protect catalase activity in cell-free assays or to inhibit Aβ-induced increases in H_2O_2 concentrations in cellular assays, to the numerous proteins, metabolites, and cellular components that may interfere with the binding of the BTA-EG_x molecules to Aβ in the cell assays. These differences may translate into the apparent requirement of a higher concentration of the BTA-EG_x molecules in the cell experiments in order to exert the same protective effects on catalase activity as seen in the cell-free enzymatic assay. Additionally, the precise intracellular concentration of catalase is not known. Differences in intracellular concentration of catalase and the concentration of catalase used in the enzymatic assay (25 nM) would make it difficult to directly and quantitatively compare the results between the cellular and cell-free experiments. Qualitatively, however, the results from the cellular and cell-free experiments are consistent with one another.

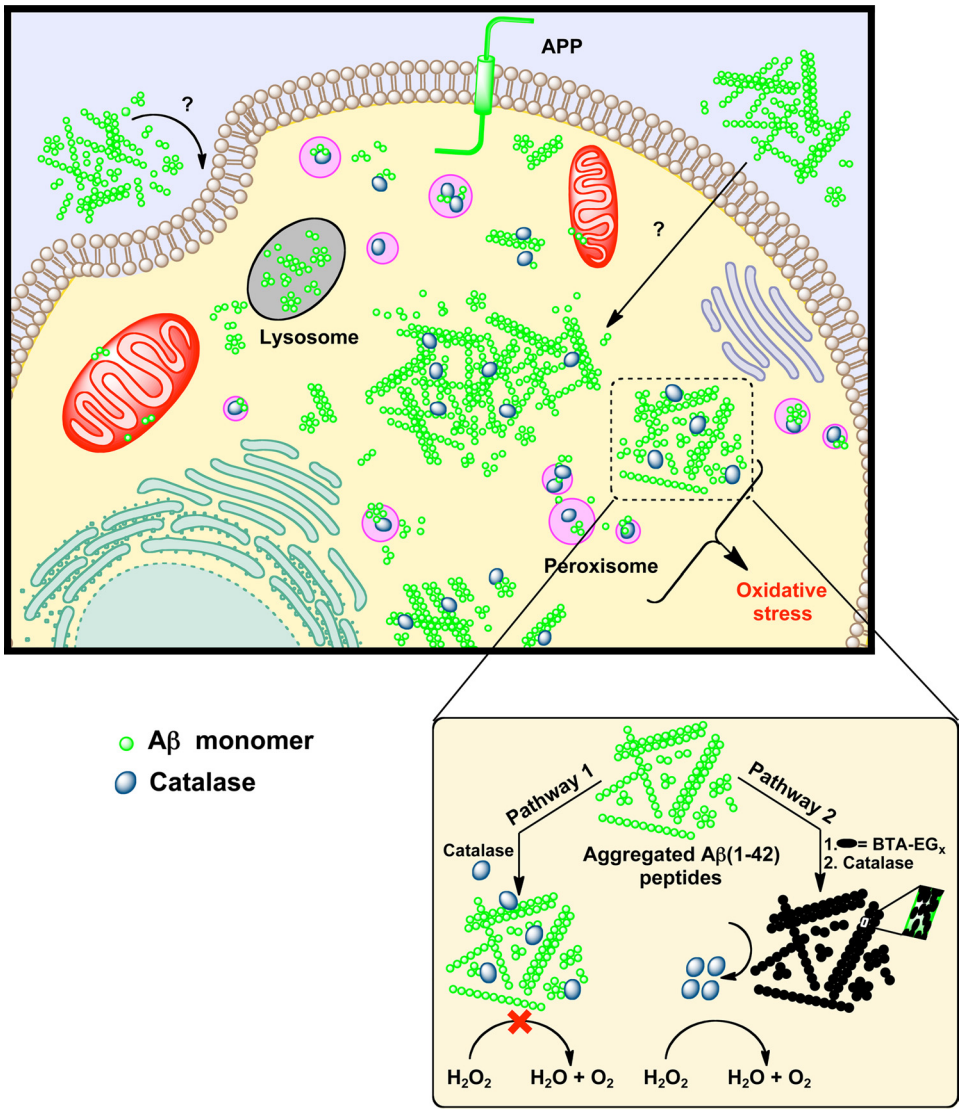

FIGURE 7. **Schematic diagram of the proposed deactivation of catalase as a contributor of Aβ-induced oxidative stress.** Cellular internalization of Aβ peptides via endocytotic and/or non-endocytotic pathways result in accumulation of Aβ within cells. The internalized Aβ can interact with proteins such as catalase present in the cytosol, peroxisomes, and other cellular organelles. The diagram of the expanded region illustrates the deactivation of the H_2O_2-degrading activity of catalase in the cytosol or peroxisomes (*pathway 1*). The BTA-EG_x molecules, however, protect the activity of catalase by forming protein-resistant surface coatings on aggregated Aβ and inhibiting harmful intracellular catalase-amyloid interactions (*pathway 2*).

To consider another possible mechanism by which the BTA-EG_x molecules could affect Aβ-catalase interactions, for instance, by affecting the aggregation state of Aβ, we performed dynamic light scattering experiments of Aβ preparations (74–76). We carried out these experiments in the presence and in the absence of the BTA-EG_x molecules and found that the aggregation states of Aβ were not altered significantly due to the presence of the BTA-EG_x molecules (see supplemental Fig. S10). In contrast, incubation of aggregated Aβ peptides with vanillin, a molecule known to inhibit Aβ aggregation (77), resulted in a population of Aβ monomers.

DISCUSSION

Aβ has been implicated as a possible causative agent for oxidative stress in AD (9, 78). Proposed mechanisms for Aβ-induced oxidative damage in cells include: 1) Aβ peptides interact directly with anti-oxidant enzymes resulting in accumulation of ROS (20–23); 2) Aβ peptides interact directly with cellular membranes resulting in uncontrolled calcium influx as a consequence of forming transient, ion channel-like pores (79–87); the resulting disruption of calcium homeostasis can lead to mitrochondrial dysfunction, followed by increased H_2O_2 production and generation of high levels of ROS (86, 88); and 3) Aβ peptides interact directly with intracellular transition metal ions such as Fe^{2+} (89–92), resulting in the catalytic reduction of O_2 to H_2O_2 in cells (17, 18, 89).

Here, we developed a small molecule probe to investigate, in detail, the first mechanism, *i.e.* the specific contribution of protein-amyloid interactions toward Aβ-induced oxidative stress. The results presented here support that deactivation of catalase by intracellular catalase-amyloid interactions can lead to Aβ-induced increases in H_2O_2 levels and to subsequent toxicity in cells. We base this conclusion on the following three key observations. First, Aβ internalized in cells and co-

localized with catalase. The results from fluorescence imaging experiments (Fig. 3 and supplemental Figs. S3–S6) demonstrate that exogenous aggregated Aβ(1–42) is capable of entering the cells through an endocytotic lysosomal pathway (67, 70, 93, 94) or a non-endocytotic pathway (95). After the initial uptake of Aβ, the Aβ peptides can accumulate in the cytosol, peroxisomes, mitochondria, and other intracellular compartments. Fig. 7 summarizes the results presented here in a graphical illustration that describes the proposed deactivation of catalase as a contributor of Aβ-induced oxidative stress. Because we found a significant fraction of Aβ co-localized with catalase in the peroxisomes and in the cytosol (25, 96) (Fig. 3*C*) and co-immunoprecipitated with catalase (Fig. 4), it is apparent that Aβ interacts directly with catalase inside of live cells (Fig. 7, *pathway 1*). Moreover, addition of small molecule inhibitors of catalase- Aβ interactions significantly reduced co-localization of Aβ and catalase inside the cells (Figs. 3, *H* and *L* and 7, *pathway 2*) without affecting significantly the uptake of Aβ in cells (Fig. 5*G*).

Second, binding interactions between catalase and Aβ deactivate catalase inside of live cells, leading to decreased degradation of H_2O_2 in solution (Fig. 6*A*) and increased cellular levels of H_2O_2 (Fig. 2*A*). The results presented here reveal that small molecule inhibitors of catalase- Aβ interactions are capable of protecting the activity of catalase in Aβ-rich solutions (Fig. 6, *B* and *C*) and of attenuating Aβ-induced increases in H_2O_2 levels in cells (Fig. 2*B*).

Third, Aβ significantly reduced cell viability (Fig. 1*A*) at concentrations that led to a 3-fold increase in cellular H_2O_2 levels (Fig. 2*A*). These results provide evidence for a correlation between Aβ-induced oxidative stress and Aβ toxicity as proposed by others (11, 13, 36). Remarkably, the BTA-EG_x molecules (by inhibiting catalase-amyloid interactions) significantly reduced the toxicity of Aβ peptides in cells (Fig. 1*B*) at concentrations that also reduced Aβ-induced increases in cellular H_2O_2 levels (Fig. 2*B*). This result further supports the important role of catalase-Aβ interactions in Aβ-induced elevations of H_2O_2 and in Aβ-mediated toxicity.

Although the results presented here clearly demonstrate that intracellular catalase-amyloid interactions induce elevations in cellular H_2O_2 levels, an important question is whether these interactions are relevant to AD pathology. The accumulation of catalase in senile plaques (41) suggests that *in vivo* environments do indeed provide evidence for binding of catalase to Aβ. We hypothesize that these *in vivo* catalase-amyloid interactions lead to deactivation of catalase, resulting in neuronal loss as a consequence of increased levels of H_2O_2 and its metabolites in the brain. This hypothesis is supported by the strong correlation of deactivation of intracellular catalase by either Aβ (Fig. 6*A*) or by catalase inhibitor 3AT (97) with the ensuing increased H_2O_2 levels (Fig. 2*A*) as well as with reduced viability (Fig. 1*B* and supplemental Fig. S11) in cells.

The results presented here provide clear evidence for the important role of catalase-amyloid interactions in Aβ-induced oxidative stress in cells, as outlined in Fig. 7. The results, however, do not rule out the possibility that amyloid interactions with proteins other than catalase could also contribute to cellular injury. We previously reported that BTA-EG_4 and BTA-EG_6 are capable of inhibiting several different Aβ-binding proteins from associating with aggregated Aβ peptides (55). It is, therefore, likely that the BTA-EG_x molecules in cells also attenuate harmful effects of Aβ on proteins other than catalase. From a therapeutic point of view, this is, of course, an attractive characteristic. Furthermore, these BTA-EG_x molecules exhibit desirable drug-like characteristics (98, 99) because they are: 1) non-toxic and cell permeable; 2) small (MW of BTA-EG_4 = 418 and MW of BTA-EG_6 = 504) and have beneficial topological polar surface areas (42, 100); 3) low in the number of H-bond donors (*i.e.* less than 5); and 4) low in the number of H-bond acceptors (*i.e.* less than 10). Most importantly, as revealed in this work, these molecules inhibit catalase- Aβ interactions, reduce the extent of co-localization of Aβ and catalase in cells, protect the activity of catalase in Aβ-rich environments, inhibit Aβ-induced increases in cellular H_2O_2 levels, and reduce Aβ toxicity. In conclusion, the formation of protein-resistant surface coatings on aggregated forms of amyloid proteins introduces an attractive and novel strategy for probing the effect of Aβ on cells and potentially for treatment of AD.

Acknowledgments—We thank Jennifer Meerloo and Dr. Kersi Pestonjamasp for technical assistance. We thank Neal Sekiya of the UCSD Flow Cytometry Research Core for acquiring the flow cytometry data and Valentina Matlachova for preliminary work in developing the catalase activity assay. We acknowledge the UCSD Cancer Center Microscopy Shared Facility supported by Grant P30 CA23100 and the UCSD Neuroscience Microscopy Shared Facility supported by Grant P30 NS047101. We also acknowledge the National Science Foundation for support of the mass spectrometry facility at UCSD (CHE-0116662).

REFERENCES

1. Harman, D. (1956) *J. Gerontol.* **11,** 298–300
2. Harman, D. (1981) *Proc. Natl. Acad. Sci. U.S.A.* **78,** 7124–7128
3. Subbarao, K. V., Richardson, J. S., and Ang, L. C. (1990) *J. Neurochem.* **55,** 342–345
4. Mecocci, P., MacGarvey, U., and Beal, M. F. (1994) *Ann. Neurol.* **36,** 747–751
5. Hensley, K., Hall, N., Subramaniam, R., Cole, P., Harris, M., Aksenov, M., Aksenova, M., Gabbita, S. P., Wu, J. F., Carney, J. M., Lovell, M., Markesbery, W. R., and Butterfield, D. A. (1995) *J. Neurochem.* **65,** 2146–2156
6. Lovell, M. A., Ehmann, W. D., Butler, S. M., and Markesbery, W. R. (1995) *Neurology* **45,** 1594–1601
7. Smith, M. A., Perry, G., Richey, P. L., Sayre, L. M., Anderson, V. E., Beal, M. F., and Kowall, N. (1996) *Nature* **382,** 120–121
8. Markesbery, W. R., and Carney, J. M. (1999) *Brain Pathol.* **9,** 133–146
9. Butterfield, D. A., Drake, J., Pocernich, C., and Castegna, A. (2001) *Trends Mol. Med.* **7,** 548–554
10. Aksenov, M. Y., Aksenova, M. V., Butterfield, D. A., Geddes, J. W., and Markesbery, W. R. (2001) *Neuroscience* **103,** 373–383
11. Behl, C., Davis, J. B., Lesley, R., and Schubert, D. (1994) *Cell* **77,** 817–827
12. Hensley, K., Carney, J. M., Mattson, M. P., Aksenova, M., Harris, M., Wu, J. F., Floyd, R. A., and Butterfield, D. A. (1994) *Proc. Natl. Acad. Sci. U.S.A.* **91,** 3270–3274
13. Schubert, D., Behl, C., Lesley, R., Brack, A., Dargusch, R., Sagara, Y., and Kimura, H. (1995) *Proc. Natl. Acad. Sci. U.S.A.* **92,** 1989–1993
14. Yan, S. D., Chen, X., Fu, J., Chen, M., Zhu, H., Roher, A., Slattery, T., Zhao, L., Nagashima, M., Morser, J., Migheli, A., Nawroth, P., Stern, D.,

and Schmidt, A. M. (1996) *Nature* **382,** 685–691
15. Behl, C. (1997) *Cell Tissue Res.* **290,** 471–480
16. Markesbery, W. R. (1997) *Free Radic. Biol. Med.* **23,** 134–147
17. Huang, X., Atwood, C. S., Hartshorn, M. A., Multhaup, G., Goldstein, L. E., Scarpa, R. C., Cuajungco, M. P., Gray, D. N., Lim, J., Moir, R. D., Tanzi, R. E., and Bush, A. I. (1999) *Biochemistry* **38,** 7609–7616
18. Huang, X. D., Cuajungco, M. P., Atwood, C. S., Hartshorn, M. A., Tyndall, J. D., Hanson, G. R., Stokes, K. C., Leopold, M., Multhaup, G., Goldstein, L. E., Scarpa, R. C., Saunders, A. J., Lim, J., Moir, R. D., Glabe, C., Bowden, E. F., Masters, C. L., Fairlie, D. P., Tanzi, R. E., and Bush, A. I. (1999) *J. Biol. Chem.* **274,** 37111–37116
19. Varadarajan, S., Yatin, S., Aksenova, M., and Butterfield, D. A. (2000) *J. Struct. Biol.* **130,** 184–208
20. Yan, S. D., Fu, J., Soto, C., Chen, X., Zhu, H., Al-Mohanna, F., Collison, K., Zhu, A. P., Stern, E., Saido, T., Tohyama, M., Ogawa, S., Roher, A., and Stern, D. (1997) *Nature* **389,** 689–695
21. Milton, N. G. N. (1999) *Biochem. J.* **344,** 293–296
22. Lustbader, J. W., Cirilli, M., Lin, C., Xu, H. W., Takuma, K., Wang, N., Caspersen, C., Chen, X., Pollak, S., Chaney, M., Trinchese, F., Liu, S. M., Gunn-Moore, F., Lue, L. F., Walker, D. G., Kuppusamy, P., Zewier, Z. L., Arancio, O., Stern, D., Yan, S. S., and Wu, H. (2004) *Science* **304,** 448–452
23. Yan, S. D., and Stern, D. M. (2005) *Int. J. Exp. Pathol.* **86,** 161–171
24. Halliwell, B. (1992) *J. Neurochem.* **59,** 1609–1623
25. Halliwell, B., and Gutteridge, J. M. (2007) *Free Radicals in Biology and Medicine*, 4th Ed., Oxford University Press, Oxford
26. Cadenas, E., and Davies, K. J. (2000) *Free Radical Biol. Med.* **29,** 222–230
27. Turrens, J. F. (2003) *J. Physiol-London* **552,** 335–344
28. Reddy, P. H. (2006) *J. Neurochem.* **96,** 1–13
29. Devi, L., Prabhu, B. M., Galati, D. F., Avadhani, N. G., and Anandatheerthavarada, H. K. (2006) *J. Neurosci.* **26,** 9057–9068
30. Manczak, M., Anekonda, T. S., Henson, E., Park, B. S., Quinn, J., and Reddy, P. H. (2006) *Hum. Mol. Genet.* **15,** 1437–1449
31. Gibson, G. E., Sheu, K. F., and Blass, J. P. (1998) *J. Neural. Transm.* **105,** 855–870
32. Casley, C. S., Canevari, L., Land, J. M., Clark, J. B., and Sharpe, M. A. (2002) *J. Neurochem.* **80,** 91–100
33. Caspersen, C., Wang, N., Yao, J., Sosunov, A., Chen, X., Lustbader, J. W., Xu, H. W., Stern, D., McKhann, G., and Yan, S. D. (2005) *FASEB J.* **19,** 2040–2041
34. Takuma, K., Yao, J., Huang, J., Xu, H., Chen, X., Luddy, J., Trillat, A. C., Stern, D. M., Arancio, O., and Yan, S. S. (2005) *FASEB J.* **19,** 597–598
35. Zhang, Z., Rydel, R. E., Drzewiecki, G. J., Fuson, K., Wright, S., Wogulis, M., Audia, J. E., May, P. C., and Hyslop, P. A. (1996) *J. Neurochem.* **67,** 1595–1606
36. Milton, N. G. N. (2004) *Drugs Aging* **21,** 81–100
37. Gsell, W., Conrad, R., Hickethier, M., Sofic, E., Frölich, L., Wichart, I., Jellinger, K., Moll, G., Ransmayr, G., and Beckmann, H. (1995) *J. Neurochem.* **64,** 1216–1223
38. Rensink, A. A., Verbeek, M. M., Otte-Höller, I., ten Donkelaar, H. T., de Waal, R. M. W., and Kremer, B. (2002) *Brain Res.* **952,** 111–121
39. Kaminsky, Y. G., and Kosenko, E. A. (2008) *Free Radical Res.* **42,** 564–573
40. Sagara, Y., Dargusch, R., Klier, F. G., Schubert, D., and Behl, C. (1996) *J. Neurosci.* **16,** 497–505
41. Pappolla, M. A., Omar, R. A., Kim, K. S., and Robakis, N. K. (1992) *Am. J. Pathol.* **140,** 621–628
42. Ertl, P., Rohde, B., and Selzer, P. (2000) *J. Med. Chem.* **43,** 3714–3717
43. Henzler, T., and Steudle, E. (2000) *J. Exp. Bot.* **51,** 2053–2066
44. Yamaguchi, H., Hirai, S., Morimatsu, M., Shoji, M., and Ihara, Y. (1988) *Acta Neuropathol.* **76,** 541–549
45. Kuo, Y. M., Emmerling, M. R., Vigo-Pelfrey, C., Kasunic, T. C., Kirkpatrick, J. B., Murdoch, G. H., Ball, M. J., and Roher, A. E. (1996) *J. Biol. Chem.* **271,** 4077–4081
46. McLean, C. A., Cherny, R. A., Fraser, F. W., Fuller, S. J., Smith, M. J., Beyreuther, K., Bush, A. I., and Masters, C. L. (1999) *Ann. Neurol.* **46,** 860–866
47. Pike, C. J., Burdick, D., Walencewicz, A. J., Glabe, C. G., and Cotman, C. W. (1993) *J. Neurosci.* **13,** 1676–1687
48. Hardy, J., and Selkoe, D. J. (2002) *Science* **297,** 353–356
49. Caughey, B., and Lansbury, P. T. (2003) *Annu. Rev. Neurosci.* **26,** 267–298
50. Lansbury, P. T., and Lashuel, H. A. (2006) *Nature* **443,** 774–779
51. Walsh, D. M., and Selkoe, D. J. (2007) *J. Neurochem.* **101,** 1172–1184
52. Bieschke, J., Siegel, S. J., Fu, Y., and Kelly, J. W. (2008) *Biochemistry* **47,** 50–59
53. Shankar, G. M., Li, S., Mehta, T. H., Garcia-Munoz, A., Shepardson, N. E., Smith, I., Brett, F. M., Farrell, M. A., Rowan, M. J., Lemere, C. A., Regan, C. M., Walsh, D. M., Sabatini, B. L., and Selkoe, D. J. (2008) *Nat. Med.* **14,** 837–842
54. Inbar, P., and Yang, J. (2006) *Bioorg. Med. Chem. Lett.* **16,** 1076–1079
55. Inbar, P., Li, C. Q., Takayama, S. A., Bautista, M. R., and Yang, J. (2006) *Chembiochem.* **7,** 1563–1566
56. Inbar, P., Bautista, M. R., Takayama, S. A., and Yang, J. (2008) *Anal. Chem.* **80,** 3502–3506
57. Maezawa, I., Hong, H. S., Liu, R., Wu, C. Y., Cheng, R. H., Kung, M. P., Kung, H. F., Lam, K. S., Oddo, S., Laferla, F. M., and Jin, L. W. (2008) *J. Neurochem.* **104,** 457–468
58. Walsh, D. M., Hartley, D. M., Kusumoto, Y., Fezoui, Y., Condron, M. M., Lomakin, A., Benedek, G. B., Selkoe, D. J., and Teplow, D. B. (1999) *J. Biol. Chem.* **274,** 25945–25952
59. Mohanty, J. G., Jaffe, J. S., Schulman, E. S., and Raible, D. G. (1997) *J. Immunol. Methods* **202,** 133–141
60. Lockhart, A., Ye, L., Judd, D. B., Merritt, A. T., Lowe, P. N., Morgenstern, J. L., Hong, G., Gee, A. D., and Brown, J. (2005) *J. Biol. Chem.* **280,** 7677–7684
61. Slaughter, M. R., and O'Brien, P. J. (2000) *Clin. Biochem.* **33,** 525–534
62. Fossati, P., Prencipe, L., and Berti, G. (1980) *Clin. Chem.* **26,** 227–231
63. Mosmann, T. (1983) *J. Immunol. Methods* **65,** 55–63
64. Tada, H., Shiho, O., Kuroshima, K., Koyama, M., and Tsukamoto, K. (1986) *J. Immunol. Methods* **93,** 157–165
65. Margoliash, E., Novogrodsky, A., and Schejter, A. (1960) *Biochem. J.* **74,** 339–348
66. Haass, C., Koo, E. H., Mellon, A., Hung, A. Y., and Selkoe, D. J. (1992) *Nature* **357,** 500–503
67. Glabe, C. (2001) *J. Mol. Neurosci.* **17,** 137–145
68. Takahashi, R. H., Milner, T. A., Li, F., Nam, E. E., Edgar, M. A., Yamaguchi, H., Beal, M. F., Xu, H., Greengard, P., and Gouras, G. K. (2002) *Am. J. Pathol.* **161,** 1869–1879
69. Langui, D., Girardot, N., El Hachimi, K. H., Allinquant, B., Blanchard, V., Pradier, L., and Duyckaerts, C. (2004) *Am. J. Pathol.* **165,** 1465–1477
70. LaFerla, F. M., Green, K. N., and Oddo, S. (2007) *Nat. Rev. Neurosci.* **8,** 499–509
71. Chance, B., Sies, H., and Boveris, A. (1979) *Physiol. Rev.* **59,** 527–605
72. Marttila, R. J., Röyttä, M., Lorentz, H., and Rinne, U. K. (1988) *J. Neural. Transm.* **74,** 87–95
73. Bolte, S., and Cordelieres, F. P. (2006) *J. Microsc.-Oxford* **224,** 213–232
74. Tomski, S. J., and Murphy, R. M. (1992) *Arch. Biochem. Biophys.* **294,** 630–638
75. Lomakin, A., Chung, D. S., Benedek, G. B., Kirschner, D. A., and Teplow, D. B. (1996) *Proc. Natl. Acad. Sci. U.S.A.* **93,** 1125–1129
76. Lomakin, A., Benedek, G. B., and Teplow, D. B. (1999) *Methods Enzymol.* **309,** 429–459
77. Necula, M., Kayed, R., Milton, S., and Glabe, C. G. (2007) *J. Biol. Chem.* **282,** 10311–10324
78. Hensley, K., Butterfield, D. A., Hall, N., Cole, P., Subramaniam, R., Mark, R., Mattson, M. P., Markesbery, W. R., Harris, M. E., Aksenov, M., Aksenova, M., Wu, J. F., and Carney, J. M. (1996) *Ann. N.Y. Acad. Sci.* **786,** 120–134
79. Arispe, N., Pollard, H. B., and Rojas, E. (1993) *Proc. Natl. Acad. Sci. U.S.A.* **90,** 10573–10577
80. Arispe, N., Rojas, E., and Pollard, H. B. (1993) *Proc. Natl. Acad. Sci. U.S.A.* **90,** 567–571

81. Bhatia, R., Lin, H., and Lal, R. (2000) *FASEB J.* **14,** 1233–1243
82. Kagan, B. L., Hirakura, Y., Azimov, R., Azimova, R., and Lin, M. C. (2002) *Peptides* **23,** 1311–1315
83. Kagan, B. L., Azimov, R., and Azimova, R. (2004) *J. Membr. Biol.* **202,** 1–10
84. Quist, A., Doudevski, I., Lin, H., Azimova, R., Ng, D., Frangione, B., Kagan, B., Ghiso, J., and Lal, R. (2005) *Proc. Natl. Acad. Sci. U.S.A.* **102,** 10427–10432
85. Lal, R., Lin, H., and Quist, A. P. (2007) *BBA-Biomembranes* **1768,** 1966–1975
86. Bezprozvanny, I., and Mattson, M. P. (2008) *Trends Neurosci.* **31,** 454–463
87. Capone, R., Quiroz, F. G., Prangkio, P., Saluja, I., Sauer, A. M., Bautista, M. R., Turner, R. S., Yang, J., and Mayer, M. (2009) *Neurotox. Res.* **16,** 1–13
88. Mattson, M. P. (2004) *Nature* **430,** 631–639
89. Schubert, D., and Chevion, M. (1995) *Biochem. Biophys. Res. Commun.* **216,** 702–707
90. Rottkamp, C. A., Raina, A. K., Zhu, X. W., Gaier, E., Bush, A. I., Atwood, C. S., Chevion, M., Perry, G., and Smith, M. A. (2001) *Free Radic. Biol. Med.* **30,** 447–450
91. Smith, M. A., Harris, P. L., Sayre, L. M., and Perry, G. (1997) *Proc. Natl. Acad. Sci. U.S.A.* **94,** 9866–9868
92. Huang, X. D., Moir, R. D., Tanzi, R. E., Bush, A. I., and Rogers, J. T. (2004) *Redox-Active Metals Neurol. Dis.* **1012,** 153–163
93. Knauer, M. F., Soreghan, B., Burdick, D., Kosmoski, J., and Glabe, C. G. (1992) *Proc. Natl. Acad. Sci. U.S.A.* **89,** 7437–7441
94. Yang, A. J., Chandswangbhuvana, D., Margol, L., and Glabe, C. G. (1998) *J. Neurosci. Res.* **52,** 691–698
95. Clifford, P. M., Zarrabi, S., Siu, G., Kinsler, K. J., Kosciuk, M. C., Venkataraman, V., D'Andrea, M. R., Dinsmore, S., and Nagele, R. G. (2007) *Brain Res.* **1142,** 223–236
96. Gaunt, G. L., and de Deduve, C. (1976) *J. Neurochem.* **26,** 749–759
97. Milton, N. G. N. (2001) *Neurotoxicology* **22,** 767–774
98. Lipinski, C. A., Lombardo, F., Dominy, B. W., and Feeney, P. J. (1997) *Adv. Drug Delivery Rev.* **23,** 3–25
99. Walters, W. P., Murcko, A., and Murcko, M. A. (1999) *Curr. Opin. Chem. Biol.* **3,** 384–387
100. Clark, D. E. (1999) *J. Pharm. Sci.* **88,** 815–821